MORPHOLOGICAL, THERMAL AND MECHANICAL PROPERTIES OF 90/10 (WT %/ WT %) PP/ABS BLENDS AND THEIR POLYMER NANOCOMPOSITES

Pravin R. Kubade[1*], Pankaj Tambe[2], Hrushikesh B. Kulkarni[2]

[1*]Production Engineering Department, KIT's College of Engineering., Kolhapur-416234, India.

[2]School of Mechanical Engineering, VIT University, Vellore -632014, India.

*Author to whom correspondence should be addressed: E-mail: pravinrkubade@gmail.com

Received: 5 August 2017; accepted 18 September 2017

ABSTRACT

Halloysite nanotubes (HNTs) are modified successfully using polyethyleneimine (PEI). The HNTs and HNTs modified using PEI filled 90/10 (wt/wt) polypropylene (PP) and acrylonitrile butadiene styrene (ABS) blends and its nanocomposites are prepared by melt mixing technique in presence of dual compatibilizer. Droplet morphology is refined in matrix as well as selective localization of HNTs modified using PEI shows increase in crystallinity of PP phase and formation of β-form of PP crystals. Uniform dispersion of HNTs modified using PEI in PP resulted in improvement in impact strength, tensile modulus and thermal stability. The enhancement in tensile strength, tensile modulus, and impact strength for 1 wt% of HNTs modified using PEI filled 90/10 (wt/wt) PP/ABS blends with dual compatibilizer are 14.9, 20 and 15%, respectively.

Keywords: Halloysite nanotubes (HNTs), Polyethyleneimine (PEI), PP/ABS Blends, Dual Compatibilization, Polymer blends.

1. INTRODUCTION

Two or more number of polymers can be blended together to modify the morphological characteristics for achieving the required properties which can further used for specific applications [1]. Enhanced Properties of the polymer blend is due to the combined effect of properties of individual polymer in the blend [2-8]. Polymer blending can also reduce the cost of product by mixing high cost polymer with low cost polymers to achieve desired properties. Polymer immiscibility is the problem faced during blending due to unfavorable thermodynamics, to solve this issue, third polymer need to be mixed in polymer blend called as compatibilizer. Compatibilizer is the substance which reduces the interface tension occurs between two immiscible polymers subsequently enhances the blending quality. Compatibilization of the polymer blends can be done by two strategies i.e. reactive and non-reactive [2-5,7].

Polypropylene (PP) is a type of thermoplastic extensively used for manufacturing plastic products [9-13] but PP possess very low impact properties. Addition of rubbery polymer in PP matrix can improve impact properties, which includes Ethylene Propylene Random Copolymer, Acrylonitrile Butadiene Styrene, Polyethylene Octane Copolymer, Ethylene Propylene Diene Monomer Rubber, Styrene-butadiene-styrene rubber [14-15]. Among this, Acrylonitrile Butadiene Styrene (ABS) contains a rubbery butadiene and styrene acrylonitrile contributes for improvement in impact strength and tensile properties respectively.

In general practices mechanical properties of polymer blends can be improved by mixing various nano fillers. Halloysite nanotubes (HNTs) is a type of nanofiller which has multi-layered structure having few hydroxyl group on its surface. HNTs can be easily dispersed in Poly Propylene polymer matrix because of chances of hydrogen bonding and van der Waals forces of attraction [16]. Aggregated dispersion will not help in property enhancement, to overcome this issue HNTs are need to be modified either covalently or non-covalently [17-20].

1.1 Structure of Halloysite Nanotubes (HNTs)

Bates et al. and Singh et al. reported that Halloysite nanotube (HNTs) have multilayer tubular structure [21-22]. HNTs are formed by wrapping of (1:1) clay layers at different geological condition due to incongruity in oxygen sharing between tetrahedral and octahedral sheets [23]. HNTs and kaolinite are chemically similar in nature having structural formula $[Al_2(OH)_4Si_2O_5 \cdot nH_2O]$, where monolayer of water molecule separates the layers as shown in Fig.1. Joussein et al, reported the dimensions of HNTs in submicron range with high aspect ratio. The inner is around 10 to 30 nm and outer diameter of tubes ranges from 40 to 70 nm. Length of HNTs varies from 0.2 to 1.5µm [24].

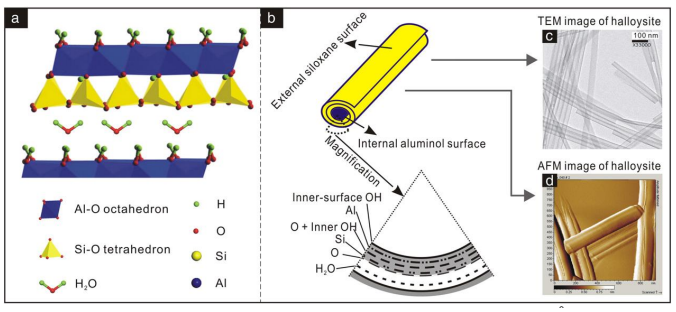

Fig. 1: Schematic diagram of (a) crystalline structure of HNTs-(10 Å), (b) structure of HNTs particle, (c, d) TEM and AFM images of HNTs [23].

HNTs are found in two polymorphs first is in hydrated form having 10 Å basal distances and another is anhydrous form of 7 Å basal distances. HNTs comprised of Al and Si in 1:1 ratio possess a molecular formula [$Al_2Si_2O_5(OH)_4 \cdot nH_2O$,] where value of n is 2 and 0 corresponds to hydrated and dehydrated HNTs [28-30]. HNTs have high aspect ratio, higher mechanical properties. HNTs are best alternatives to carbon nanotubes (CNTs) which can be used as a filler material in polymer matrix. HNTs are cheaper in cost than CNTs. In addition, HNTs disperses easily in polymers as compared to montmorillonite, fumed silica and CNTs, because of HNTs rod-like geometry and intertubular contact area is also very less [20-23]. HNTs have few hydroxyl groups and surface modification of HNTs may provide uniform dispersion in the polymer matrix. Table 1 show the typical analysis data of HNTs.

HNTs was commonly used as bioreactor [22], time-release capsule [23], and catalysts for polymer degradation [24], template [31-32], and high-tech ceramic applications [33].

Table 1: Typical analysis data of HNTs [35].

Chemical formula	Al2Si2-O5(OH)4·nH2O
Length	0.2-2 µm
Outer diameter	40-70 nm
Inner diameter	10-40 nm
Aspect ratio (L/D)	10-50
Elastic modulus (theoretical value)	140 GPa (230-340 GPa)
Mean particle size in aqueous solution	143 nm
Particle size range in aqueous solution	50-400 nm
BET surface area. (Pasbakhshet al. (2013))	22.1-81.6 m^2/g
Pore space	14-46.8%
Lumen space	11-39%
Density	2.14-2.59 g/cm^3
Average pore size	79.7-100.2 Å
Structural water release temperature	400-600 ºC

1.2 Covalent and Non Covalent modification of HNTs

To enhance the dispersion of HNTs in polymer matrix, Surface treatment of HNTs is carried out. Covalently and non-covalently modification of the HNTs can be done by exploiting the hydroxyl groups which are already present on the surface of HNTs.

Pal et al., have reported the improved dispersion of HNTs in polymer blend and localization of HNTs between two phases after surface treatment of HNTs. The performance of nanocomposites was improved due to uniform dispersion of HNTs after surface treatment [34]. HNTs surface was treated using polyethyleneimine (PEI). The Fig. 2 shows the schematic of reaction takes place between HNTs and PEI. The schematic shows an interaction of negatively charged OH group of HNTs with H atom of aNH2 functional group of PEI resulting in the grafting of PEI over HNTs.

Liu et al. [35] have modified the HNTs using 2,2(1,2-ethenediyldi-4,1-phenylene) bisbenzoxazole as there is electron transfer interactions between 2,2(1,2-ethenediyldi-4,1-phenylene) bisbenzoxazole and HNTs. Nitrogen and Oxy-

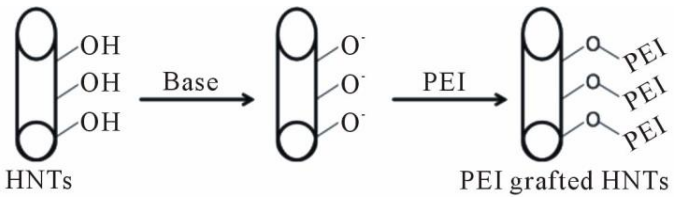

Fig. 2: Schematic representation of the surface treatment of HNTs [34].

gen atoms of EPB has a lone pair of electrons, which is accepted by the metal atoms of HNTs upon heating. Pasbaksh et al. [36] demonstrates the layer coating of γ-methacry losypropyltrimethylsilane (MPS) on HNTs surface. Carli et al. 2014 used various silane coupling agent to modify HNTs in view to enhance the interaction between HNTs and poly(hydoxybutyrate-co-hydroxyvalerate) (PHBV). Silane coupling agent forms a layer around HNTs and end amine function group of silane coupling agent interacts with PHBV. Khunova et al. [37] reported the effect of modification of HNTs by using (hexadecyl tri methyl ammonium bromide) (HEDA), urea. The HNTs was treated in 5% solution of HEDA at 80 ºC for 24 hrs. and dried in hot air oven at 60 ºC for 24 hrs. after filtration process and further ground and sieved again. The urea was intercalated into HNT by grinding process. The (10g mixture) clay and urea (2:1 in proportion) were mixed with the help of planetary mill for 30 min and 374 rpm rotation speed. An enhancement in mechanical properties was found using modified HNTs.In addition modification of HNT by γ-metacryloxypropyl-trimethoxysilane results in enhanced thermal stability and reduction is flammability of polymer composites was reported by Du et al. [38].

Covalent grafting of N-cyclohexyl-2-benzothiazole sulfonamide (CBS) was carried out using melt mixing. CBS/PP when melt mixed, CBS decomposes and yields benzothiazolesulfide radical. This benzothiazole sulfide radical interacted with PP radicals generated during melt processing. Benzothiazole sulfide radicals are capable of donating electrons to HNTs. Thus PP-grafted benzothiazole sulfide interacted with HNTs through electron transferring [39].
Various researcher have studied the effect of dual compatibilization on polymer blends [4,34,35,35,37]. Enhanced electrical conductivity of multiwalled carbon nanotubes (MWNTs) mixed in PP/ABS blends and polymer composites was observed due to dual compatibilization. Reactive compatibilization of polystyrene (PS) and Poly ethylene terephthalate (PET) and blends using dual compatibilization shows higher viscosity and enhanced mechanical properties. Similar results was observed in PP and Poly butyelene terephthalate blend [34]. Bonda et al. [41] studied the effect of dual compatibilization on mechanical properties of PP/ABS blends by styrene grafted maleic anhydrite (SEBS-g-MA) and polypropylene grafted maleic anhydrite (PP-g-MA) and Styrene-ethylene, butylene-styrene [42].
In present work, HNTs are considered as naofiller material

to improve crystallinity, mechanical and thermal behavior of PP and ABS blends by using two types of compatibilizer such as SEBS-g-MA and PP-g-MA. HNTs are modified via branched polyethyleneimine (PEI) to enhance the distribution of HNTs in PP/ABS.

2. EXPERIMENTAL

2.1 Materials

Polypropylene is procured from Reliance Industries Ltd, India. HNTs were kindly supplied by Imerys Tableware, New Zealand. Polypropylene grafted maleic anhydride (PP-g-MA) was obtained from Pluss Polymer Ltd, India. ABS was purchased from Strylotion, India under the trade name Terluran GP-22. SEBS-g-MA was bought from Karton, India. PP/ABS blends and their composites was prepared using counter rotating twin screw extruder (S. C. Dey & Co., India) at 155–210–240 °C with a rotational speed of 10 rpm with various HNTs concentrations

2.3 Composite Preparation

Initially, 1 g of HNTs was mixed with 400 ml of distilled water using probe ultrasonication for 30 min. To maintain the solution pH to 8–9, NaOH solution was added. Thereafter, 4 ml of branched PEI solution was added in the ultrasonicated HNTs in distilled water under constant magnetic stirring. The magnetic stirring of resultant solution was carried out at 60 °C for 24 h. Then the branched PEI-treated HNTs was centrifuged for 10 min at 6000 rpm. Centrifuged HNTs modified using branched PEI were washed with distilled water, further dried in vacuum at 80 °C. Final product is called as mHNTs.

HNTs-filled polymer blend were prepared using counter rotating twin screw extruder (S. C. Dey & Co., India) at 155°C –210°C –24°C with 10 rpm rotational speed with a fixed concentration of HNTs (3 wt.%). The codes and composition of different specimens are shown in Table 1. Injection moulding samples was prepared using mini injection moulding machine operated at a temperature of 230 °C, holding time of 3 min and at an applied pressure of 8 bar.

2.4 Material and Composite Characterization

HNTs morphology was characterized by high resolution transmission electron microscopy (HRTEM JEOL JEM 2100). XRD (D8 Advance, BRUKER) is used to study the crystal structure of HNTs. XRD patterns were recorded between 5° and 80° (2θ) with a step of 0.02°. Tensile testing of nanocomposites were tested using universal testing machine (Instron (8801)) with ASTM D638 standard. Impact testing of HNTs-filled nanocomposites specimens were tested using CEAST (Instron) tester using ASTM D256 standard on un-notched specimens. TGA of HNTs-filled polymer blend was performed on (Q500 TA instruments) at heating rate of 10 °C/min in temperature range 25–900 °C. The amount of the sample used is 6–8 mg. Differential scanning calorimetric (DSC) of HNTs-filled polymer blend were carried at heating–cooling–heating run for all samples were recorded in the temperature range from 25 °C to 235 °C at a scan rate of 10 °C /min.The degree of crystallinity (Xc) of PP phase was calculated from the ratio of normalized heat of fusion (ΔHm, norm) of second heating run to the heat of fusion of 100% crystalline PP, (ΔHm)100%, which was taken as 207 J/g.

3. RESULTS AND DISCUSSION

3.1 Morphology Development

Fig. 3 shows SEM micrographs of Kryo-fractured and etched pure blend (PASP), 1 wt. % of HNT (PASP+1wt%. HNTs) and branched PEI modified HNTs filled 90/10 (wt%/wt%) PP/ABS blends and their composites in existence of PP-g-MA and SEBS-g-MA (PASP+1wt%. mHNTs). Addition of PASP+1wt%. HNTs and PASP+1wt%. mHNTs results in refined morphology as compare to PASP.

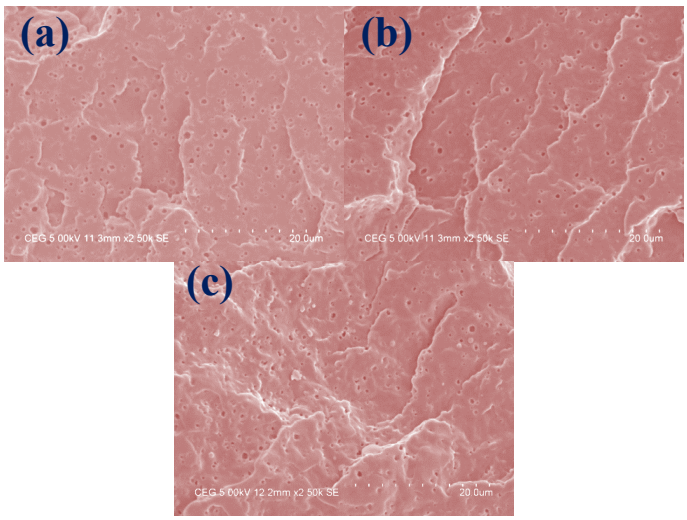

Fig. 3: SEM micrographs of cryofractured and etched (a) PASP (b) PASP+1 wt. % HNTs (c) PASP+1 wt. % mHNTs

Mechanical behaviour of polymer blends and its composites are not only affected by Dn, but also by the interparticle distance (ID). ID of polymer blends and its composites can be calculated using following formula [43,44].

$$ID = d\left[\left(\frac{k\pi}{6v_A}\right)^{1/3} - 1\right] \quad (1)$$

Where, V_A is volume fraction of dispersed phase, d is diameter of dispersed phase, k=1 for cubic packing. The ID of HNTs filled PP/ABS blends and its composites were calculated.

Average droplet diameter (D_n) was calculated manually taking average of all the droplet diameters from the SEM image as per scale mentioned in image. Whereas the interparticle distance was calculated with the help of the turner equation as above.

Average diameter of distributed phase (D_n) and distance between particle (ID) of pure blend and PASP+1wt%. HNTs and PASP+1wt%. mHNTs is shown in Table 2. ID

decreases remarkably in case of 1 wt% of PASP+1wt%. mHNTs.

Table 2: Average diameter of dispersed phase and interparticle distance of PASP, PASP+1wt%. HNTs, PASP+1wt%. mHNTs

Sr. No.	Sample Codes	Dn (µm)	ID (µm)
1	PASP	0.51	0.19
2	PASP+1wt%. HNTs	0.42	0.16
3	PASP+1wt%. mHNTs	0.38	0.15

3.2 Crystallization Studies

DSC was used to characterize the crystalline behaviour of PASP+1wt%. HNTs and PASP+1wt%. mHNTs. Table 3. Show the crystallization and melting parameters of PASP+1wt%. HNTs and PASP+1wt%. mHNTs. Fig. 4a shows the crystallization exotherms of PASP+1wt%. HNTs and PASP+1wt%. mHNTs. The crystallization temperature (T_c) of PASP is 121.4 °C. With an addition of PASP+1wt%. HNTs show an increase in T_c. The increase in T_c is due to heterogeneous nucleating effect of HNTs for PP crystals formation. Modification of HNTs leads to further increase in T_c of PASP+1wt%. mHNTs. The increase in T_c depict the heterogeneous nucleating effect of branched PEI modified HNTs on PP.

Table 3: Melting and crystallization parameters of PASP, PASP+1wt%. HNTs, PASP+1wt%. mHNTs

Sr. No.	Sample Codes	T_m (°C)	$(\Delta H_m)_{nor}$ (J/g)	X_c (%)	T_c (°C)
1	PASP	162.9	74.66	36.1	121.4
2	PASP+1wt%. HNTs	163.7	97.81	47.2	122.1
3	PASP+1wt%. mHNTs	163.7	81.01	39.1	122.7

Table 4: Average diameter of dispersed phase and interparticle distance of PASP, PASP+1wt%. HNTs, PASP+1wt%. mHNTs

Sr. No.	Sample Codes	Dn (µm)	ID (µm)
1	PASP	0.51	0.19
2	PASP+1wt%. HNTs	0.42	0.16
3	PASP+1wt%. mHNTs	0.38	0.15

Fig. 4b shows the melting endotherm of PASP+1wt%. HNTs and PASP+1wt%. mHNTs. All melting endotherm shows a single melting peak. The melting temperature (T_m) of PASP is 162.9 °C. With an addition of PASP+1wt%. HNTs and PASP+1wt%. mHNTs shows an increase in T_m. The increase in Tm depict an enhancement in crystallinity of PASP+1wt%. HNTs and PASP+1wt%. mHNTs. The calculated value of percent crystallinity of PASP+1wt%. HNTs and PASP+1wt%. mHNTs is shown in Table 4. Crystallinity of PP phase of PASP is 36.1%. Addition of PASP+1wt%. HNTs results in an increase in crystallinity of PP phase to 47.2 %. The increase in crystallinity of

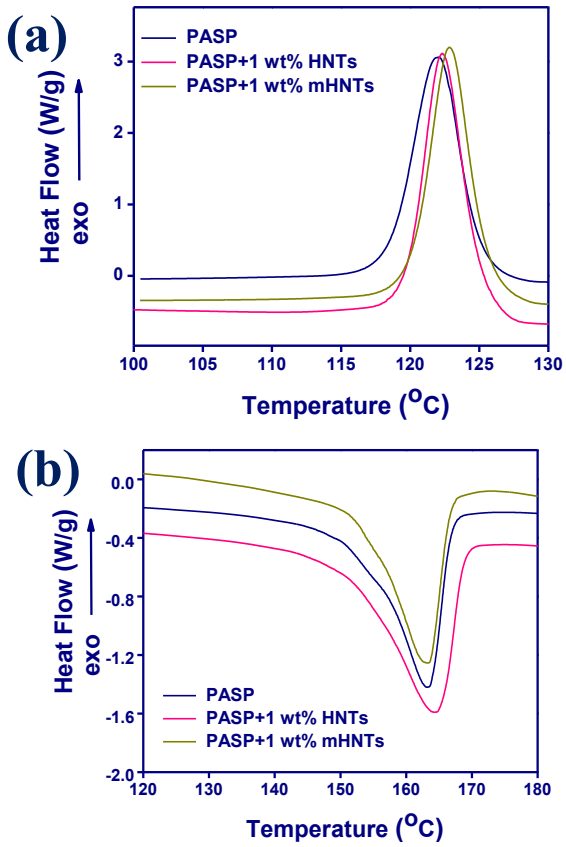

Fig. 4: DSC (a) crystallization exotherms and (b) melting endotherms of PASP, PASP+1wt%. HNTs and PASP+1wt%. mHNTs

PP phase is due to refinement of morphology and dispersion of high aspect ratio HNTs; as the droplet size reduces, higher surface area of contact in between matrix and droplet phase contributing more nucleating sites. Further, PASP+1wt%. mHNTs results in an increase in crystallinity of PP phase to 39.1 %. But, PP phase crystallinity of PASP+1wt%. mHNTs is less as compare to PASP+1wt%. HNTs. The decrease of PP phase crystallinity is due to the enhanced dispersion of branched PEI modified HNTs, and over which huge amount of amorphous PP chains are adsorbed.

3.3 Mechanical Behaviour

It is well known that refinement in dispersed phase morphology influence the mechanical behaviour of polymer blends. The refinement in dispersed phase morphology in case of PASP+1wt%. mHNTs can significantly influence the mechanical properties. Fig. 5 and 6 shows the tensile behavior of PASP and PASP+1wt%. mHNTs. Tensile strength and tensile modulus increased to maximum by an addition of PASP+1wt%. mHNTs, and thereafter, tensile strength and tensile modulus decreases at higher concentration of branched PEI modified HNTs as discussed in previous work [12,13]. The significant increase in mechanical properties is highest at PASP+1wt%. mHNTs are due to lowest droplet diameter of ABS dispersed phase and interparticle distance in between dispersed ABS droplets. In addition, the enhancement is due to improved dispersion of PASP+1wt%. mHNTs, and at higher concentration of

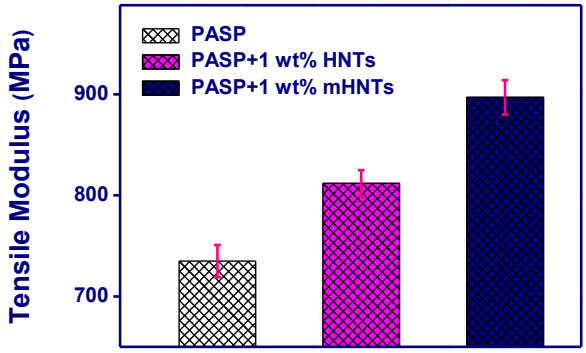

Fig. 5: Tensile modulus of PASP, PASP+1wt%. HNTs, PASP+1wt%. mHNTs

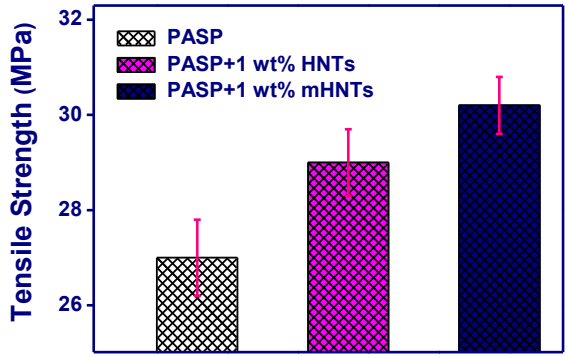

Fig. 6: Tensile strength of PASP, PASP+1wt%. HNT,s PASP+1wt%. mHNTs

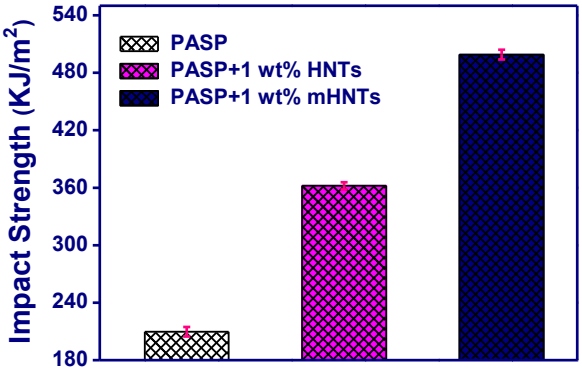

Fig. 7: Impact strength of PASP, PASP+1wt%. HNTs, PASP+1wt%. mHNTs

branched PEI modified HNTs, tensile strength and tensile modulus decreases due to aggregation of PASP+1wt%. mHNTs [12,13].

The refinement in dispersed droplet morphology also influences the impact properties of polymer blends significantly. Thus, refinement in dispersed droplet morphology of PASP+1wt%. mHNTs have a significant influence over the impact properties. Fig. 7 shows the impact behavior of PASP and PASP+1wt%. mHNTs. The maximum increase in impact strength is at PASP+1wt%. mHNTs, and impact strength decreases at higher concentration of PASP+1wt%. mHNTs [12,13]. The significant increase in impact strength at PASP+1wt%. mHNTs are due to refinement in ABS droplet diameter of dispersed phase and decrease in interparticle distance between dispersed ABS droplets. In addition, the impact strength increases due to enhanced dispersion of PASP+1wt%. mHNTs, and at higher concentration, impact strength decreases due to aggregated dispersion of PASP+1wt%. mHNTs [12,13].

Fig. 8 shows the impact fractured SEM image of PASP+1wt%. HNTs and PASP+1wt%. mHNTs. The fracture images do not show the formation of fibrils depicting the brittle fracture.

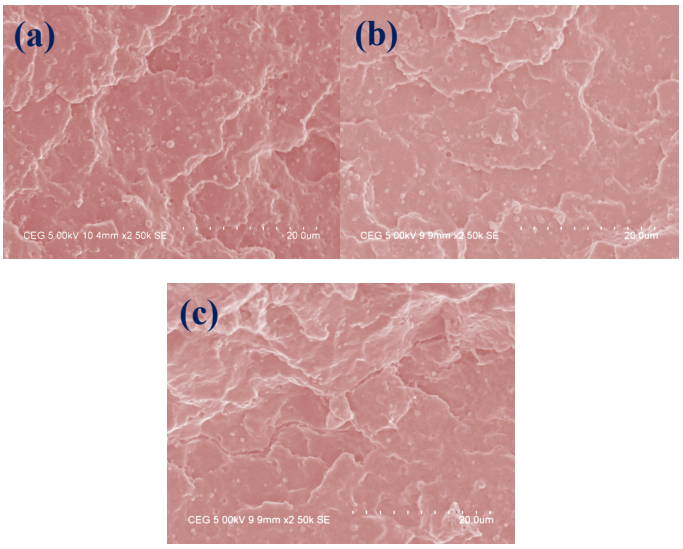

Fig 8: Impact fractured SEM micrographs of (a) PASP (b) PASP+1 wt% HNTs (c) PASP+1 wt% mHNTs

3.4 Thermal Behaviour

It is expected that with an enhanced dispersion of filler in polymer blend matrix result in an improved thermal stability. So, addition of PASP+1wt%. mHNTs should enhance the thermal stability. TGA was carried out to characterize the thermal behaviour of PASP+1wt%. HNTs and PASP+1wt%. mHNTs. Fig. 9a show the thermogravimetric (TG) curves and Fig. 9b show the differential thermogravimetric (DTG) curves of PASP+1wt%. HNTs and PASP+1wt%. mHNTs. Thermal stability enhances by an addition of HNTs in PASP. In addition, thermal stability further enhances by an addition of PASP+1wt%. mHNTs. The improvement in thermal stability is due to the high interfacial area of contact in between HNTs and polymer. In case of PASP+1wt%. mHNTs, the contact interfacial area is more as compare to unmodified HNTs in PASP and PASP+1wt%. mHNTs. Thus, PASP+1wt%. mHNTs show highest enhancement in thermal stability.

4. SUMMARY AND CONCLUSIONS

PASP+1wt%. HNTs and PASP+1wt%. mHNTs shows enhanced crystallinity of PP phase as compare to. HNTs and PASP+1wt%. mHNTs shows the formation of matrix-droplet morphology. Average droplet diameter and interparticle distance of PASP+1wt%. mHNTs is lower as compare to PASP and PASP+1wt%. HNTs. Due to refinement in morphology results in a remarkable improvement in tensile modulus and impact strength of PASP+1wt%. mHNTs is lower as compare to PASP and PASP+1wt%. HNTs. In

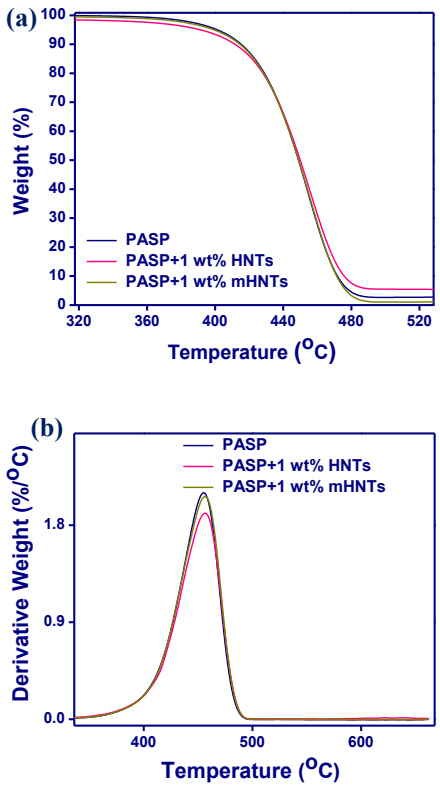

Fig. 9: (a) TGA and (b) DTG curves of PASP, PASP+1wt%. HNTs, PASP+1wt%. mHNTs

addition, thermal stability also enhances for PASP+1wt%. mHNTs as compare to PASP and PASP+1wt%. HNTs.

In conclusion, PASP+1wt%. mHNTs shows highest enhancement in tensile and impact properties as compared to previous published literature which makes it suitable for application where impact load is the major consideration while designing the product.

References:

1. **Mekroud, A., D. Benachour, and S. Bensaad,** "Influence of organoclay filler on the properties of polystyrene/low-density polyethylene blend", Composite Interfaces, 22/9 (2015), 809-822.
2. **Jogi, B. F., et al,** "The simultaneous addition of styrene maleic anhydride copolymer and multiwall carbon nanotubes during melt mixing on the morphology of binary blends of polyamide6 and acrylonitrile butadiene styrene copolymer", Polymer Engineering & Science, 55/2 (2015), 457-465.
3. **Panda, Biswajit, Arup R. Bhattacharyya, and Ajit R. Kulkarni,** "Ternary polymer blends of polyamide 6, polypropylene, and acrylonitrile butadiene styrene: Influence of multiwalled carbon nanotubes on phase morphology, electrical conductivity, and crystallization", Polymer Engineering & Science, 51/8 (2011), 1550-1563.
4. **Khare, Rupesh A., et al.,** "Dispersion of multiwall carbon nanotubes in blends of polypropylene and acrylonitrile butadiene styrene", Polymer Engineering & Science, 51/9 (2011), 1891-1905.
5. **Khare, Rupesh A., Arup R. Bhattacharyya, and Ajit R. Kulkarni.** "Melt mixed polypropylene/acrylonitrile butadiene tyrene blends with multiwall carbon nanotubes: Effect of compatibilizer and modifier on morphology and electrical conductivity", Journal of applied polymer science, 120/5 (2011), 2663-2672.
6. **Hom, Sheleena, et al.,** "PP/ABS blends with carbon black: morphology and electrical properties", Journal of applied polymer science, 112/2 (2009), 998-1004.
7. **Khare, Rupesh A., et al.**, "Influence of multiwall carbon nanotubes on morphology and electrical conductivity of PP/ABS blends", Journal of Polymer Science Part B: Polymer Physics, 46/21 (2008), 2286-2295.
8. **Bose, Suryasarathi, et al.,** "Influence of multiwall carbon nanotubes on the mechanical properties and unusual crystallization behavior in melt mixed co continuous blends of polyamide6 and acrylonitrile butadiene styrene", Polymer Engineering & Science, 49/8 (2009), 1533-1543.
9. **Tambe, Pankaj B., et al.,** "Structure–property relationship studies in amine functionalized multiwall carbon nanotubes filled polypropylene composite fiber", Polymer Engineering & Science, 52/6 (2012), 1183-1194.
10. **Tambe, Pankaj B., Arup R. Bhattacharyya, and Ajit R. Kulkarni.**, "The influence of melt mixing process conditions on electrical conductivity of polypropylene/multiwall carbon nanotubes composites", Journal of Applied Polymer Science, 127/2 (2013), 1017-1026.
11. **Khare, Rupesh A., et al.,** "Dispersion of multiwall carbon nanotubes in blends of polypropylene and acrylonitrile butadiene styrene", Polymer Engineering & Science, 51/9 (2011), 1891-1905.
12. **Kubade, Pravin, and Pankaj Tambe.,** "Influence of halloysite nanotubes (HNTs) on morphology, crystallization, mechanical and thermal behaviour of PP/ABS blends and its composites in presence and absence of dual compatibilizer", Composite Interfaces, 23/5 (2016), 433-451.
13. **Kubade, Pravin, and Pankaj Tambe.,** "Influence of surface modification of halloysite nanotubes and its localization in PP phase on mechanical and thermal properties of PP/ABS blends", Composite Interfaces, 24/5 (2017), 469-487.
14. **Tang, Tao, and Baotong Huang.,** "Compatibilization of polypropylene/poly (ethylene oxide) blends and crystallization behavior of the blends", Journal of Polymer Science Part B: Polymer Physics, 32/12 (1994), 1991-1998.
15. **Balakrishnan, Harintharavimal, et al.,** "Epoxidized natural rubber–toughened polypropylene/organically modified montmorillonite nanocomposites", Journal of Thermoplastic Composite Materials, 27/2 (2014), 233-250.
16. **Ning, Nan-ying, et al.,** "Crystallization behavior and mechanical properties of polypropylene/halloysite composites", Polymer, 48/25 (2007), 7374-7384.
17. **Prashantha, K., et al.,** "Mechanical behaviour and essential work of fracture of halloysite nanotubes filled polyamide 6 nanocomposites", Composites Science and Technology, 71/16 (2011), 1859-1866.
18. **Prashantha, K., M. F. Lacrampe, and P. Krawczak.,** "Processing and characterization of halloysite nanotubes filled polypropylene nanocomposites based on a masterbatch route: effect of halloysites treatment on structural and mechanical properties", Express Polymer Letters, 5/4 (2011), 295-307.
19. **Liu, Mingxian, et al.,** "Halloysite nanotubes as a novel β-nucleating agent for isotactic polypropylene", Polymer, 50/13 (2009), 3022-3030.
20. **Liu, Mingxian, et al.,** "Benzothiazole sulfide compatibilized polypropylene/halloysite nanotubes composites", Ap-

plied Surface Science, 255/9 (2009), 4961-4969.
21. Bates, Thomas F., Fred A. Hildebrand, and Ada Swineford., "Morphology and structure of endellite and halloysite", American Mineralogist, 35/7-8 (1950), 463-484.
22. **Singh, Balbir,** "Why Does Halloysite Roll?--A New Model", Clays and Clay Minerals, 44/2 (1996), 191-196.
23. **Yuan, Peng, Daoyong Tan, and Faïza Annabi-Bergaya.,** "Properties and applications of halloysite nanotubes: recent research advances and future prospects", Applied Clay Science, 11/2 (2015), 75-93.
24. **Joussein, E., et al.,** "Halloysite clay minerals–a review", Clay minerals, 40/4 (2005), 383-426.
25. **Guimaraes, Luciana, et al.,** "Structural, electronic, and mechanical properties of single-walled halloysite nanotube models", The Journal of Physical Chemistry C, 114/26 (2010), 11358-11363.
26. **Du, Mingliang, Baochun Guo, and Demin Jia.,** "Newly emerging applications of halloysite nanotubes: a review", Polymer International, 59/5 (2010), 574-582.
27. **Du, Mingliang, et al.,** "Effects of halloysite nanotubes on kinetics and activation energy of non-isothermal crystallization of polypropylene", Journal of polymer research, 17/1 (2010), 109.
28. **Shchukin, Dmitry G., et al.,** "Halloysite nanotubes as biomimetic nonreactors", Small, 1/5 (2005), 510-513.
29. **Lvov, Yuri M., et al.,** "Halloysite clay nanotubes for controlled release of protective agents", Acs Nano, 2/5 (2008), 814-820.
30. **Cho, Kyo-Hyun, et al.,** "Performance of pyrophyllite and halloysite clays in the catalytic degradation of polystyrene", Reaction Kinetics and Catalysis Letters, 88/1 (2006), 43-50.
31. **Wang, Aiping, et al.,** "Synthesis of mesoporous carbon nanosheets using tubular halloysite and furfuryl alcohol by a template-like method", Microporous and Mesoporous Materials, 108/1 (2008), 318-324.
32. **Zhang, Long, and Peng Liu.,** "Facile fabrication of uniform polyaniline nanotubes with tubular aluminosilicates as templates", Nanoscale Research Letters, 3/8 (2008), 299.
33. **Sumi, Katsuhiro, Yuichi K, and Etsuro KATO.,** "Preparation of dense cordierite ceramics from ultrafine particles of magnesium hydroxide and kaolin", Journal of the Ceramic Society of Japan, 106/1235 (1998), 693-697.
34. **Pal, Parthajit, et al.,** "Mechanical and crystalline behavior of polymeric nanocomposites in presence of natural clay", Open Journal of Applied Sciences, 2/04 (2012), 277.
35. **Liu, Mingxian, et al.,** "The Role of Interactions between Halloysite Nanotubes and 2, 2 [variant prime]-(1, 2-Ethenediyldi-4, 1-phenylene) Bisbenzoxazole in Halloysite Reinforced Polypropylene Composites", Polymer journal, 40/11 (2008), 1087.
36. **Pasbakhsh, Pooria, et al.,** "EPDM/modified halloysite nanocomposites", Applied Clay Science, 48/3 (2010), 405-413.
37. **Khunova, V., et al.,** "The effect of halloysite modification combined with in situ matrix modifications on the structure and properties of polypropylene/halloysite nanocomposites", Express Polymer Letters, 7/5 (2013), 471-479.
38. **Du, Mingliang, Baochun Guo, and Demin Jia,.** "Thermal stability and flame retardant effects of halloysite nanotubes on poly (propylene)", European Polymer Journal, 42/6 (2006), 1362-1369.
39. **Liu, Mingxian, et al.,** "Halloysite nanotubes as a novel β-nucleating agent for isotactic polypropylene", Polymer, 50/13 (2009), 3022-3030.
40. **Shieh, Yeong Tarng, Tzong Neng Liao, and Feng Chih Chang.,** "Reactive compatibilization of PP/PBT blends by a mixture of PPgMA and epoxy resin", Journal of applied polymer science, 79/12 (2001), 2272-2285.
41. **Bonda, Sateesh, Smita Mohanty, and Sanjay K. Nayak.,** "Influence of compatibilizer on mechanical, morphological and rheological properties of PP/ABS blends", Iranian Polymer Journal, 23/6 (2014), 415-425.
42. **Guo, Baochun, et al.,** "Thermoplastic Elastomers Derived from Scrap Rubber Powder/LLDPE Blend with LLDPE graft (Epoxidized Natural Rubber) Dual Compatibilizer", Macromolecular Materials and Engineering, 289/4 (2004), 360-367.
43. **Borggreve, R. J. M., et al.,** "Brittle-tough transition in nylon-rubber blends: effect of rubber concentration and particle size", Polymer, 28/9 (1987), 1489-1496.
44. **Jiang, Ruhong, et al.,** "Dietary plasma protein is used more efficiently than extruded soy protein for lean tissue growth in early-weaned pigs", The Journal of nutrition, 130/8 (2000), 2016-2019.